# MR Study of Water Exchange and Cell Membrane Permeability in Rat Liver Cells Using a Tissue-Specific MR Contrast Agent

Yongmin Chang[1], Yong Sun Kim[1], Sang Kwon Lee[1], Hun Kyu Ryeom[1], Jong Min Lee[1], Kyung Jin Suh[1], Yong Joo Kim[1], Duk Sik Kang[1], Robert Clarkson[2]

**Purpose** : A precise NMR technique for measuring the rate of water exchange and cell membrane permeability across the hepatocyte membrane using liver-specific MR contrast agent is described.

**Materials and Methods** : The rat hepatocytes isolated by perfusion of the livers were used for the NMR measurements. All experiments were performed on an IBM field cycling relaxometer operating from 0.02 MHz to 60 MHz proton Larmor frequency. Spin-echo pulse sequence was employed to measure spin-lattice relaxation time, T1. The continuous distribution analysis of water proton T1 data from rat hepatocytes containing low concentrations of the liver specific contrast agent, Gd-EOB-DTPA, modeled by a general two compartment exchange model.

**Results** : The mean residence time of water molecule inside the hepatocyte was approximately 250 msec. The lower limit for the permeability of the hepatocyte membrane was $(1.3 \pm 0.1) \times 10^{-3}$ cm/sec. The CONTIN analysis, which seeks the natural distribution of relaxation times, reveals direct evidence of the effect of diffusive exchange. The diffusive water exchange is not small in the intracellular space in the case of hepatocytes.

**Conclusions** : Gd-EOB-DTPA, when combined with continuous distribution analysis, provides a robust method to study water exchange and membrane permeability in hepatocytes. Water exchange in hepatocyte is much slower than that in red blood cells. Therefore, tissue-specific contrast agent may be used as a functional agent to give physiological information such as cell membrane permeability.

**Index words** : Paramagnetic contrast agents ; Tissue-specific agents ; Hepatocyte ; Permeability ; Relaxation time

## Introduction

An understanding of water exchange between extracellular and intracellular compartments, especially in the presence of a paramagnetic contrast agent (PCA), is required to evaluate MR images of complex tissues, such as the liver. In particular, analysis of tissue relaxation in terms of multiple relaxation components may improve tissue charac-

**JKSMRM 2 : 73-82(1998)**
[1] Department of Diagnostic Radiology, College of Medicine, Kyungpook National University and Hospital
[2] Illinois EPR Center, College of Medicine, University of Illinois at Urbana-Champaign
Received april 10, 1998 ; revised August 3, 1998 ; accepted August 20, 1998
Address reprint requests to : Yongmin Chang Ph.D., Department of Diagnostic Radiology, College of Medicine, Kyungpook National University and Hospital, # 50 Samduk-dong, Taegu, 700-412, Korea. Tel. 82-53-420-5471, Fax. 82-53-422-2677

terization(1, 2) as well as provide fundamental information concerning the interplay of diffusion rate, membrane permeability and compartment size(3, 4). Multi-component relaxation of protons reflects the heterogeneity or compartmentalization of tissue. The apparent relaxation components, which are measurable, depend on both the intrinsic relaxation times of the compartments and the effects of exchange between compartments. A robust method of analysis for understanding multi-component relaxation in compartmentalized system is crucial in this context.

Historically, the two main techniques used to study water exchange across the biological membrane have been radioactive tracer and nuclear magnetic resonance (NMR). Due to their relative simplicity and availability, erythrocytes have been a major target for such studies(5—7). Other mammalian cells have not been studied as extensively. The advantages of NMR over the tracer method were extensively discussed elsewhere(8). Among several NMR approaches suggested, one simple and direct method uses the fact that the extracellular relaxation time can be shortened with a paramagnetic ion. Most studies utilizing this approach have made use of extracellular agents, with the assumption that the contrast agent is impermeable to the cell membrane. The disadvantage of extracellular agents is that they need to be used in high concentration (〉10 mM), even for agents showing high relaxivity. For a biological system showing relatively slow exchange between compartments, this high concentration is unable to measure the water exchange rate accurately due to the dominant contribution of one of the apparent compartment fractions.

In the MR method, multi-component relaxation is traditionally interpreted using non-linear least square(NLLS) methods based on a multi-exponent model. This method needs to make a priori assumptions about the character and the components of the relaxation. However, the exact number of components in complex biological samples is difficult to model correctly because spins may experience many different environments during the measurements. Even in cases where a multi-exponential model accounts satisfactorily for the data, relaxation times and the estimates of component size derived from this fitting are very sensitive to noise as well as to the range and baseline of the experimental data. One example is the observation that small changes in the time range of the measured data cause large variations in the estimates of the relaxation times even with a large number of data points(22).

In this paper, we used Gd-Ethoxybenzyl(EOB)-DTPA as a contrast agent for water exchange studies in hepatocytes. The agent, which is gadolinium diethylenetriaminepentaacetic acid covalently linked to the lipophilic ethoxybenzyl moiety, is an MR contrast agent(9, 10). Recently, Gd-EOB-DTPA was shown to be a potential candidate for functional hepatobiliary MR imaging(11). That is, this liver-specific contrast agent is taken up by hepatocytes and subsequently eliminated through the biliary system. For water exchange experiments, this uptake by hepatocytes makes it possible to observe the apparent fraction of both compartments, one of which would be negligibly small and unobservable if only extracellular agents were employed. Thus, the water exchange measurement on hepatocytes can be done efficiently and accurately with moderate concentration (〈2 mM) of Gd-EOB-DTPA, allowing the detection of a biexponential T1 distribution in vivo.

For the analysis of such experimental data, we employed a continuous distribution(CONTIN) method based on the Inverse Laplace Transformation technique instead of the conventional non-linear least square fitting model. CONTIN analysis makes no a priori assumptions about the character and the components of the relaxation and will calculate the natural distribution of relaxation times in the biological system(12, 13). This probability distribution of different values of relaxation times was recently termed a relaxogram by Labadie et al(26). Information on the relaxation distribution is of critical importance in the study of water diffusion. Since the conventional discrete exchange model assumes a sharp boundary between compartments, models of this kind assume that all the spins in each compartment are equal. If, however, diffusion through the membrane affects the exchange between two compartments, the variation in the time that is necessary for a spin to diffuse will consequently result in a distribution of relaxation times. Thus, the CONTIN method has a great advantage in investigating the effects of diffusive exchange in many biological situations.

## Theory

### A. Two Compartment Exchange Model

For suspensions of rat hepatocytes, we refer to the extracellular compartment as compartment A, characterized by Pa, $T_{1a}$, and $\tau_a$. The intracellular compartment is assigned as compartment B with its characteristic $P_b$, $T_{1b}$, and $\tau_b$. Here Pa and Pb are the intrinsic fractional sizes of compartments A and B; $T_{1a}$ and $T_{1b}$ are intrinsic longitudinal relaxation times and $\tau_a$ and $\tau_b$ are the mean residence times for exchangeable water molecules. All intrinsic quantities are those that would be measured in the absence of exchange between the two compartments. The detailed theory for this model, based on the modified Bloch equations, has been described(14, 15). The results show that the normalized time-dependent magnetization M(t), arising from the two-site system, is described by*

$$M(t) = P_a^* \exp(-t/T_{1a}^*) - P_b^* \exp(-t/T_{1b}^*) \qquad [1]$$

where $T_{1a}^*$ and $T_{1b}^*$ are apparent relaxation times, and $P_a^*$ and $P_b^*$ are measured apparent fractions of water in the extracellular and intracellular space. These quantities can be given as functions of the intrinsic parameters:

$$P_a^* = \frac{1}{2} - \frac{1}{4C^*}[(P_b - P_a)(\frac{1}{T_{1a}} - \frac{1}{T_{1b}}) - \frac{1}{\tau a} + \frac{1}{\tau b}] \qquad [2]$$

$$P_b^* = 1 - P_a^* \qquad [3]$$

$$\frac{1}{T_{1a}^*} = C + C^* \qquad \frac{1}{T_{1b}^*} = C - C^* \qquad [4]$$

$$C = \frac{1}{2}(\frac{1}{T_{1a}} + \frac{1}{T_{1b}} + \frac{1}{\tau_a} + \frac{1}{\tau_b}) \qquad [5]$$

$$C^* = \frac{1}{2}\sqrt{(\frac{1}{T_{1a}} - \frac{1}{T_{1b}} + \frac{1}{T_{\tau a}} - \frac{1}{T_{\tau b}})^2 + \frac{4}{\tau_a \tau_b}} \qquad [6]$$

The same equations will also hold true for the transverse relaxation times T2 as long as there is no significant chemical shift difference between the two sites. Three quantities ($T_{1a}^*$, $T_{1b}^*$ and $P_a^*$ or $P_b^*$) can be obtained from the experiment, whereas four unknown quantities ($T_{1a}$, $T_{1b}$, $P_a$ or $P_b$ and $\tau_a$ or $\tau_b$) are required to describe the two-site exchange model completely. From the general equation (Eq. [1]) for the two-site exchange model, we can derive several interesting limiting cases.

#### 1) Slow exchange limit

When the water exchange times ($\tau_a$ and $\tau_b$) are infinite, the intracellular and extracellular water will relax independently. The observed relaxation behavior is a double exponential with $P_a^* = P_a$, $T_{1a}^* = T_{1a}$, $P_b^* = P_b$ and $T_{1b}^* = T_{1b}$.

#### 2) Fast exchange limit

In the opposite limiting case ($\tau_a$, $\tau_b \ll T_{1a}$, $T_{1b}$), $P_a^*$ becomes vanishingly small and the relaxation curve is single exponential

$$M(t) = \exp[-t(\frac{P_a}{T_{1a}} + \frac{P_b}{T_{1b}})] \qquad [7]$$

The fast exchange limit shows that the observed relaxation is independent of the exchange rate and the multi-component relaxation behavior is masked by the exchange.

#### 3) Dilute paramagnetic ion case

When the relaxation time of the water at site A is much shorter than that of site B ($T_{1a} \ll T_{1b}$) due to the presence of paramagnetic ions, the observed relaxation decay is single exponential

$$M(t) \simeq \exp(-t/T_{1b}^*) \qquad [8]$$

$$\frac{1}{T_{1b}^*} = \frac{1}{T_{1b}} + (\frac{P_a}{P_b})(\frac{1}{T_{1a} + \tau_a}) \qquad [9]$$

To arrive to this result, the detailed balance condition $P_a/\tau_a = P_b/\tau_b$ is assumed. Physically, the longer observable relaxation time depends on both the value of the shorter relaxation time and the exchange rate. If we assign the site A to bound water of the paramagnetic metal complex, then T1a has a Larmor frequency dispersion (Nuclear Magnetic Resonance Dispersion) controlled by Solomon-Bloembergen-Morgan theory(16, 17). Eq. (9) was also obtained by Swift and Connick and others(18, 19). They arrived at the same result by solving eigenvalue equations of the Bloch-McConnell equations.

### B. Continuous distribution analysis

In this study, we employed the CONTIN analysis developed by Provencher(12, 13). This FORTRAN computer program is an approach that seeks a continuous distribution of relaxation times(relaxogram) using the Inverse Laplace Transform(ILT) technique. The basic observation is that the Laplace Transform (LT) is the fundamental relation between a set of relaxation data, f(t), and the probability distribution $\rho$(T) of relaxation times that describe those data(20, 21). Thus, the Laplace Transform f(t) is defined by

$$f(t)=L[\rho(T)]=\int_0^\infty \rho(T)\,F(t,T)\,dT \qquad [10]$$

where t can be the decay time of the experimental data and the time T refers to relaxation times T1 or T2. The standard expression of the LT is appreciated when the integral kernel F(t, T)=exp(−t/T). it is then obvious that the ILT of f(t) is the continuous relaxation time distribution $\rho$(T):

$$\rho(T)=L^{-1}[f(t)] \qquad [11]$$

Unlike the case for the Fourier Transform(FT) and its inverse transform, the ILT is a mathematically ill-conditioned problem, which means that a solution of ILT has unbounded errors. Experimentally, this means that ILT is quite sensitive to noise in any real relaxation data. With progress in modern numerical inversion techniques, several practical approaches for computing the ILT problem have been described in the literature(21, 26). One of the most promising approach is CONTIN. This program adopts a strategy which uses the fewest degrees of freedom that are necessary for a given data set. This is the principle of parsimony. The principle states that of all the possible solutions, the most appropriate solutions are the simplest ones, i.e., the ones that may not have all the detail of the true solution, but which contain the detail that is necessary to fit the data. Thus, the most parsimonious solution is less likely to be an artifact. By seeking a continuous distribution, another major advantage of CONTIN is that it allows the analysis to determine the nature of the relaxation components without any a priori assumptions about the nature of these components. Thorough tests of this program using simulated and real data sets have been reported by several groups (22, 23). We performed our own tests of CONTIN to confirm the validity of the program.

## Materials and Methods

### A. Experimental

Hepatocytes were isolated from rats(Sprague-Dawley, 250g) by perfusion of the liver with collagenase(27). The cells were used for the NMR measurements immediately after isolation. Ghosts of equine erythrocytes were prepared according to the protocol described by Dodge et al(29). Gd-EOB-DTPA was provided by Schering, AG(Berlin). A stock solution of Gd-EOB-DTPA(20 mM) was made and diluted accordingly to give 1.0, 1.5, 2.0 and 2.5 mM solutions. All experiments were performed on an IBM field cycling relaxometer(Biomedical Magnetic Resonance Laboratory, University of Illinois at Urbana-Champaign) operating from 0.02 MHz to 60 MHz proton Larmor frequency. The relaxometer uses a spin echo(90−180) pulse sequence to measure T1. The basic design of this multi-frequency spectrometer was described elsewhere(24). The existing program that runs the spectrometer typically takes 16 data points for determining T1 at each magnetic field value. This NMR relaxation data, the relaxation curve, when obtained over a rather limited time domain, could appear to be fit by a single exponential model. To avoid this problem and to make use of the novel continuous distribution method, we reprogrammed the software to take 100 decay measurements at each field value as well as extending the time domain to approximately 4 times the value of the longest T1.

### B. Data Analysis

The raw T1 relaxation data were analyzed using CONTIN, which provides a continuous T1 relaxation time distribution. All CONTIN analyses were done on a VAX station 3500 running VMS 5.3 version. For a typical CONTIN analysis, the regularizor parameter ($\alpha$) was fixed to all data sets by assuming that noise does not vary significantly to produce changes in $\alpha$. This means that the noise level does not change dramatically from one data set to another. CONTIN analysis reveals three apparent quantities($T_{1a}^*$, $T_{1b}^*$ and $P_a^*$ or $P_b^*$) from the relaxation measurement. However, to describe the two-site exchange model completely, four unknown quant-

ities($T_{1a}$, $T_{1b}$, $P_a$ or $P_b$ and $\tau_a$ or $\tau_b$) are required. Therefore, we need to know at least one of these independently. The other three parameters can then be derived by using either curve fitting techniques or analytical solutions. In practice, the intrinsic(i.e., without exchange) extracellular T1 is determined independently using simulation. One can choose an intrinsic extracellular T1 value which gives the best agreement between experiment and simulation, particularly the positions of the maxima in the T1 distribution. Mathematically, we now have three independent equations with three parameters. Therefore, the three remaining parameters can be found by seeking the analytical solutions of the exchange equations. Maple(Waterloo Maple Software, Waterloo, CANADA), which is a symbolic computation software running on a SUNSparc station(Sun Microsystem, CA), was used as the platform to find the analytical solutions. Two-site exchange simulations were performed using a FORTRAN simulation program written in our department and under Maple.

## Results

Figure 1 shows the T1 relaxogram from a sample of hepatocytes (Fig. 1(A)) and from a sample of RBC ghosts (Fig. 1(B)), both containing with 1 mM Gd-EOB-DTPA. The insets are typical T1 relaxation data points(filled circles) taken at 50 MHz for these suspensions. The solid lines represent the effective Laplace transforms of the relaxograms. Both show the high quality of the fitting of these data. A typical $\alpha$ value for these relaxogram was $6.6 \times 10^{-5}$. The hepatocytes/Gd-EOB-DTPA sample shows two peaks in T1 space, whereas only one peak is seen for the RBC ghost/Gd-EOB-DTPA sample at the same contrast agent concentration.

Due to the effect of water exchange, the observed peak positions and relative fractions can be significantly different from the intrinsic values. For the hepatocyte suspension, the peak with the smaller value of T1 was assigned to the extracellular water signal and the larger T1 value to intracellular signal. The continuous distribution analysis revealing two peaks in the T1 distribution strongly suggests two biological compartments with relatively slow water exchange between them. However, the result from the RBC ghost sample seems to suggest fast exchange between compartments. The water exchange time in RBC preparations is known to be approximately 20 msec(5).

As explained earlier in the Data Analysis section, by assuming that the intrinsic extracellular T1 is not

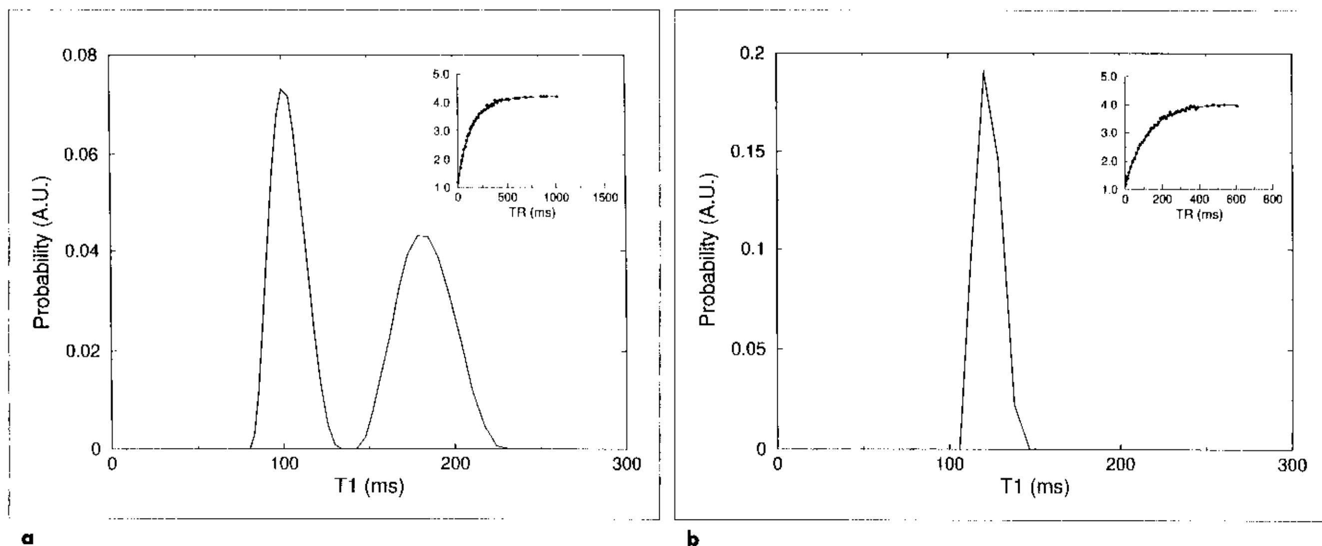


**Fig. 1.** Continuous distribution analysis of 1 mM Gd-EOB-DTPA in rat hepatocyte sample (**a**). The T1 distribution from the sample at 50 MHz shows two distinct peaks arising from two different biological compartments. The apparent T1's (peak positions) are different from the intrinsic T1's of the two compartments due to water exchange between them. (**b**) is a T1 relaxogram from a sample of RBC ghosts containing 1 mM Gd-EOB-DTPA. Only single peak is observed due to fast exchange between two compartments. The insets are T1 relaxation data points(filled circles). The solid lines represent the effective Laplace Transform of the corresponding relaxograms.

much different from that of the cell-free solution, we calculated the analytical solutions. After discarding unphysical solutions(those with negative relaxation times or negative exchange times), the calculated water exchange time of the hepatocyte was found to be 250 msec. The other parameters found simultaneously are the intrinsic fraction of the extracellular population ($P_a$=0.87) and the intrinsic intracellular T1 (=500 msec). These values seem to be quite reasonable. The intracellular population ($P_b = 1 - P_a$) was calculated using the cell diameter and the number of cells. The value was within $\pm$ 15 % of the $P_b$ determined from the our analysis.

The measurement of intrinsic intracellular T1 in the absence of a PCA is not straightforward. The simplest technique is to measure a packed cell sample without doped paramagnetic ions. However, it should be noted that a measurement on such a sample would include a contribution from the trapped plasma volume. Therefore, the measurement of packed hepatocyte cell samples provides only a rough estimation of the intrinsic intracellular T1 and our data suggest that it is normally longer than 1000 msec. The enhancement of the relaxation of the intracellular water as determined by our method suggests an uptake of contrast agent by hepatocytes. This agrees with the observations made by other groups who have shown that Gd-EOB-DTPA is a hepatobiliary agent(9 – 11). Also, an EPR study of the rotational dynamics of EOB-DTPA complexed to vanadyl(which has been shown to be dynamically similar to Gd-EOB-DTPA) shows the evidence of small uptake of the agent(30).

Figure 2 shows a stacked plot of the T1 relaxogram obtained from the experiment in which samples of hepatocytes were suspended in solutions of various concentrations of Gd-EOB-DTPA (1.0 – 2.5 mM). The abscissa gives the longitudinal relaxation time values. The oblique axis reports the extracellular contrast agent concentration. The third axis represents the probability of T1 in arbitrary units. By adding more contrast agent, the apparent extracellular signal (the peak at shorter T1 values) shifts progressively to lower values, but in a nonlinear fashion. The intracellular water signal appeared to shift much less in peak position within the concentration range studied. The other observation is that there is a relative increase in the area of the extracellular peak and a relative decrease in the area of the intracellular peak as one adds more contrast agent. These facts clearly manifest the effects of water exchange, and are in agreement with the predictions from the two-site exchange model(Eq. (2) – (6)). Also, the two-site exchange model shows that if the intrinsic intracellular T1($T_{1b}$) becomes shorter by increasing the concentration of paramagnetic agent in the intracellular volume, the apparent intracellular peak position should shift to lower T1 values. Our result showing unshifted intracellular peak positions seems thus to suggest a saturation effect for Gd-EOB-DTPA uptake by hepatocytes. However, the exact amount of uptake needs to be

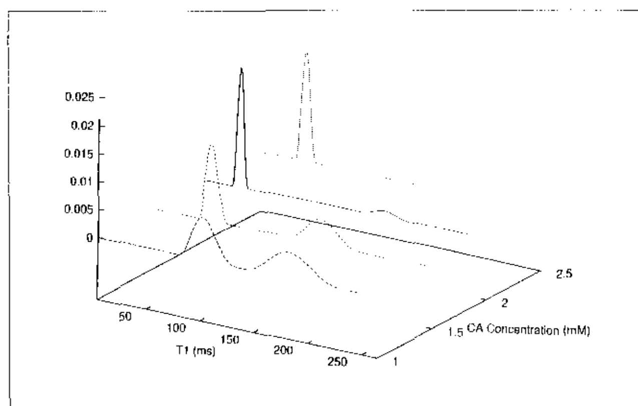


**Fig. 2.** A stacked plot of the T1 distributions obtained from the experiment. The samples of hepatocytes were suspended in solutions with different concentrations of Gd-EOB-DTPA. The abscissa gives the longitudinal relaxation time(T1) value. The oblique axis reports the paramagnetic contrast agent concentration.

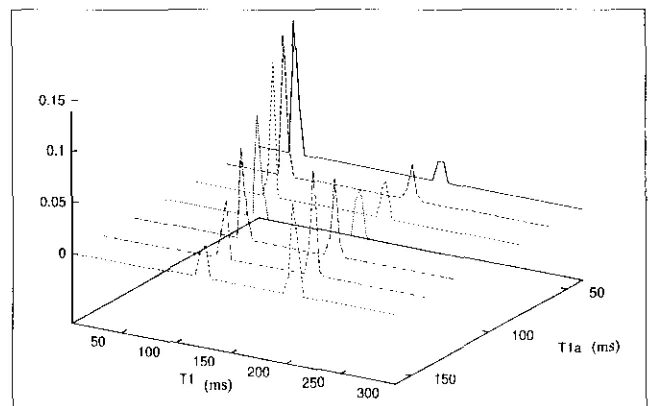


**Fig. 3.** A stacked plot of the T1 distributions resulting from a simulation based on the two-site exchange model. The oblique axis gives the intrinsic T1 of extracellular space (compartment A). The extracellular T1's were chosen from 40 msec to 160 msec to simulate approximately the same concentration of Gd-EOB-DTPA as in the experiment.

investigated quantitatively.

It is quite important to test the validity of the determined parameters. That is, if the parameters are correctly determined and if the underlying assumptions in the analysis are reasonable ones, the simulation based on the two-site exchange model should reproduce the same results as the experiment. Figure 3 shows a simulated T1 relaxogram stacked plot with parameter values obtained from our analysis. The oblique axis, which represents the intrinsic T1 of extracellular space, is equivalent to that of Figure 2. The extracellular T1's ranging from 140 msec to 40 msec were used to simulate approximately the same concentrations of Gd-EOB-DTPA as in the experiment. The relaxogram in which extracellular T1 was arranged to be 120 msec corresponds to that of the 1 mM concentration in Fig. 2. When we compare both experiment and simulation based on the two-site exchange model, the agreement is quite good. The main results of Fig. 2 and 3 are : (1) one can discriminate the extracellular water from the intracellular water using modest concentrations of the liver-specific agent, Gd-EOB-DTPA ; (2) the two-site chemical exchange model describes the experiment well with some degree of water diffusion. This is a quite interesting finding because there is a controversy about the validity of the chemical exchange model for understanding exchange between tissue compartments. Detailed discussion will be given in the next section.

## Discussion and Conclusion

Multi-component relaxation is normally interpreted using a chemical exchange model based on discrete exchange between compartments. This discrete model assumes that all protons in each compartment are equivalent and can be described by a single exchange time. In other words, the water protons in each compartment are well mixed and there is no memory about the diffusional history. In many studies of RBC suspensions, this model was successful(6 -- 8). However, there has been growing interest to include the effects of water diffusion(25). Diffusive exchange models make use of the diffusion equation to account for the spatial aspects of relaxation. Therefore, the magnetization vector M becomes a function of position as well as a function of time. The diffusive model is obviously a more general approach, but its application to find an exact solution in the arbitrary geometry of a cell membrane presents difficulties. Also the diffusive exchange model is currently limited to one dimensional analysis.

The main message from the diffusive model is that a continuous distribution of relaxation times should

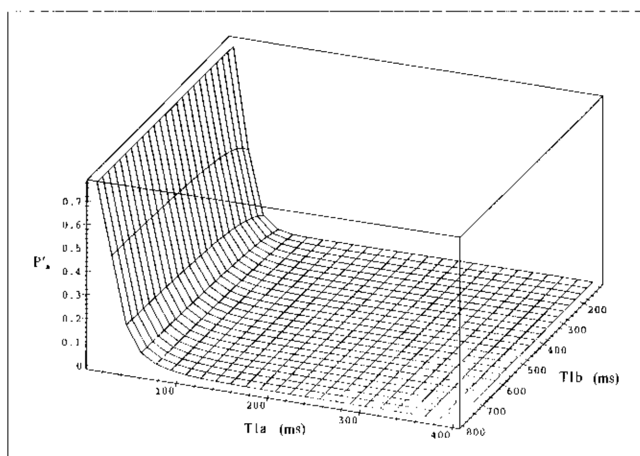


**Fig. 4.** Simulation of the apparent population($P_a^*$) of compartment A. The water exchange time is 20 msec as in the case of RBC. The population of compartment B is $P_b^* = 1 - P_a^*$. $T_{1a}$ and $T_{1b}$ are intrinsic T1 relaxation times at compartment A and B respectively. For 1 mM Gd-EOB-DTPA in RBC ghost suspension, $T_{1a}$ is 120 msec. $P_a^*$ is negligibly small at this $T_{1a}$ value regardless of the value of $T_{1b}$. Thus only single peak appears in the continuous distribution analysis.

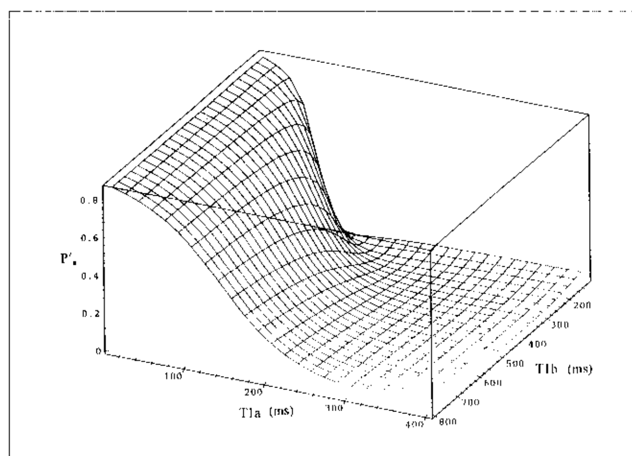


**Fig. 5.** Simulation of the apparent population($P_a^*$) with an exchange time of 250 msec as in the case of hepatocytes. $T_{1a}$ is 120 msec at 1 mM Gd-EOB-DTPA. $T_{1b}$ is estimated as 500 msec from the analytical solutions. $P_a^*$ is approximately 0.5 at these value. $P_b^*$ is then 0.5. Thus two distinct peaks(seen in Fig. 1(a)) appeared, having nearly the same apparent populations in the 1 mM Gd-EOB-DTPA/hepatocyte sample.

be observable along with the degree of diffusion. Our method has a natural advantage over nonlinear least squares(NLLS) methods, because CONTIN analysis seeks a continuous distribution of relaxation times. Comparing Fig. 2 and 3, the experimental results appeared to have a broader T1 distribution than the simulated one. The simulation was based on the discrete exchange model. The broadening of the intracellular water peak is especially noticeable. This may indicate that the relaxation of intracellular water is partly controlled by diffusion. That is, water protons near the membrane show relaxation behavior different from the protons more distant from the cell membrane. Therefore, the diffusive exchange effect may not be small in the case of hepatocytes.

Our results show that the water exchange rate of hepatocytes is slow. The exchange time determined by our experiment is 250 msec. In comparison, the reported exchange time of RBC suspension is approximately 20 msec(5). CONTIN analysis did not show two peaks in the case of RBC ghosts containing with 1 mM Gd-EOB-DTPA, in agreement with this faster exchange. From our results on both hepatocytes and RBC ghosts, we can conclude that the water exchange times are much different for these two types of cells. The simulations for the apparent fraction of the extracellular population($P_a^*$) support our conclusion. Figure 4 shows the simulated apparent extracellular fraction for an RBC ghost suspension containing with 1 mM Gd-EOB-DTPA. At this concentration, the intrinsic extracellular T1($T_{1a}$) is 120 msec. $P_a^*$ is negligibly small at this T1a value regardless of the intrinsic intracellular T1($T_{1b}$). Thus, $P_b^*$ is dominant and only a single peak, resulting from the intracellular population, is expected to be seen in the experiment. To increase the apparent fraction of the extracellular population, simulation suggests that high concentrations of the paramagnetic agent would be necessary. This explains why most previous exchange experiments on RBC systems required high concentrations of paramagnetic ions. This observation is a consequence of exchange between the two compartments, a result that underscores the validity of our simulations and approach. The simulation for hepatocytes with the same concentration of Gd-EOB-DTPA is shown in Fig. 5. With an exchange time of 250 msec, $P_a^*$ reached almost 0.5. Thus, two distinct peaks appeared, having nearly equal fractions in the 1 mM Gd-EOB-DTPA/hepatocytes sample. It is also interesting to note that the apparent fraction ($P_a^*$ or $P_b^*$) is sensitive to the intrinsic intracellular T1. As $T_{1b}$ becomes shorter, the slope of $P_a^*$ becomes steeper along the $T_{1b}$ axis. The permeability coefficient of the cell membrane can be estimated from(26)

$$P=\frac{V}{A\tau_i} \quad [12]$$

where $\tau_i$ is the average exchange time of water in a compartment. P also depends on the volume V and surface area A of the cell. For simplicity, we assume that the hepatocyte is spherical (V/A=r/3). Using the mean radius of rat hepatocyte(r=9.6 $\pm$ 0.9 $\mu$m)(27, 28) and the exchange time obtained from our experiment, the estimated permeability coefficient P is (1.3 $\pm$ 0.1) $\times 10^{-3}$ cm/sec. For human RBC, the reported permeability coefficient was approximately 4.7 $\times 10^{-3}$ cm/sec. Even though the hepatocyte is larger than RBC in size, the hepatocyte membrane appears to be more restrictive of water exchange between the intracellular and the extracellular compartments than the RBC membrane.

In conclusion, we have shown that Gd-EOB-DTPA, when combined with our continuous distribution analysis, provides a robust method to study water exchange in hepatocytes. CONTIN analysis also reveals how diffusion affects the two-site exchange model. Water exchange in hepatocytes is much slower than that in RBCs. Based on our study, we believe that tissue-specific contrast agents may be used as a tool to study compartmental water exchange. In an in vivo situation, tissue-targeted agents could provide one way of studying water exchange, avoiding the need for high paramagnetic agent concentrations that are required when extracellular agents are employed.

## References

1. Kroeker RM, Stewart CA, Bronskill MJ, Henkelman RM. Continuous distributions of NMR relaxation times applied to tumors before and after therapy with X-rays and cyclophosphamide. Magn Reson Med 1988; 6: 24-36
2. Bradamante S, Barchiesi E, Pilotti S, Borasi G. High-resolution 1H NMR spectroscopy in the diagnosis of breast cancer. Magn Reson Med 1988; 8: 440-449

3. Brownstein KR, Tarr CE. Importance of classical diffusion in NMR studies of water in biological cells. Phys Rev A 1979; 19: 2446-2453
4. Belton PS, Mills BP. The effects of diffusive exchange in heterogeneous systems on NMR line shapes and relaxation processes. Mol Phys 1987; 61: 999-1018
5. Herbst MD, Goldstein JH. A review of water diffusion measurement by NMR in human red blood cells. Am J Physiol 1989; 256: C1097
6. Fabry ME, Eisenstadt M. Water exchange between red cells and plasma: measurement by nuclear magnetic relaxation. Biophys J 1975; 15: 1101
7. Conlon T, Outhred R. Water diffusion permeability of erythrocytes using an NMR technique. Biochim Biophys Acta 1972; 288: 354
8. Belton PS, Ratcliffe RG. NMR and compartmentation in biological tissues. Prog NMR Spectr 1985; 17: 241-279
9. Schuhmann-Giampieri G, Schmitt-Willich H, Press WR et al. Preclinical evaluation of Gd-EOB-DTPA as a contrast agent in MR imaging of the hepatobiliary system. Radiology 1992; 183: 59-64
10. Weinmann H, Schuhmann-Giampieri G et al. A new lipophilic Gadolinium chelate as a tissue specific contrast medium for MRI. Magn Reson Med 1991; 22: 233-237
11. Schmitz SA, Muller A, Wagner S, Wolf K. Functional hepatobiliary imaging with Gadolinium-EOB-DTPA. Invest Radiol 1996; 31: 154-160
12. Provencher SW. A constrained regularization method for inverting data represented by linear algebraic or integral equations. Comput Phys Commun 1982; 27: 213-227
13. Provencher SW. A general purpose constrained regularization program for inverting noisy linear algebraic or integral equations. Comput Phys Commun 1982; 27: 229-242
14. Woessner DE. Nuclear transfer effects in nuclear magnetic resonance pulse experiments. J Chem Phys 1961; 35: 41-48
15. Hazelwood CF, Chang DC, Nichols BL, Woessner DE. Nuclear magnetic resonance transverse relaxation times of water protons in skeletal muscle. Biophys J 1974; 14: 583-606
16. Solomon I. Relaxation processes in a system of two spins. Phys Rev 1955; 99: 559-565
17. Bloembergen N, Morgan LO. Proton relaxation times in paramagnetic solutions: effects of electron spin relaxation. J Chem Phys 1961; 34: 842-850
18. Swift TJ, Connick RE. NMR relaxation mechanism of 17O in aqueous solutions of paramagnetic cations and the life time of water molecules in the first coordination sphere. J Chem Phys 1962; 37: 307-319
19. McLaughlin AC, Leigh JS. Relaxation times in systems with chemical exchange: approximate solutions for the nondilute case. J Magn Reson 1973; 9: 296-304
20. Overloop K, Gerven LV. NMR relaxation in absorbed water. J Magn Reson 1992; 100: 303-315
21. Stepanek P. Dynamic light scattering. In Brown W eds. 1st ed. Oxford: Clarendon Press, 1993
22. Kroeker RM, Henkelman RM. Analysis of biological NMR relaxation data with continuous distributions of relaxation times. J Magn Reson 1986; 69: 218-235
23. Lee JH. Magnetic resonance studies of tissue 23Na and 1H2O signals. Ph. D. dissertation, State University of New York 1993
24. Koenig SH, Brown RD. NMR spectroscopy of cells and organism In Gupta RK eds. 1st ed. CRC Press, 1987
25. Santyr GE, Kay I, Henkelman RM, Bronskill MJ. Diffusive exchange analysis of two compartment T2 relaxation of red blood cell suspensions containing gadolinium. J Magn Reson 1990; 90: 500-513
26. Labadie C, Lee JH, Vetek G, Springer CS. Relaxographic Imaging. J Magn Reson B 1994; 105: 99-112
27. Bacic G, Alameda JC, Iannone A, Magin RL, Swartz HM. NMR study of water exchange across the hepatocyte membrane. Magn Reson Imaging 1989; 7: 411-416
28. Cooper RL, Chang DB, Young AC, Martin CJ, Ancker-Jonson B. Restricted diffusion in biological systems. Biophys J 1974; 14: 161-177
29. Dodge JT, Mitchell CD, Hanahan DJ. The preparation and chemical characteristics of Hemoglobin-free ghosts of human serum erythrocytes. Arch Biochem Biophys 1963; 100: 119
30. Chen JW, Norby SW, Chang Y, Belford RL, Clarkson RB. Characterizing Rotational dynamics of EOB-DTPA in Isolated rat hepatocytes. XVIIth International Conference on Magnetic Resonance in Biological Systems, Keystone 1996

대한자기공명의과학회지 2:73－82(1998)

# 조직 특정 MR 조영제를 이용한 쥐의 간세포막의 물분자 교환 및 투과율의 MR 측정기법

장용민[1], 김용선[1], 이상권[1], 염헌규[1], 이종민[1], 서경진[1], 김용주[1], 강덕식[1], Robert Clarkson[2]

[1]경북대학교 의과대학 진단방사선과학교실

[2]Illinois EPR Center, College of Medicine, University of Illinois at Urbana-Champaign

**목 적**: 간특정 MR 조영제를 이용하여 간세포의 세포막을 통한 물분자의 교환 및 세포막 투과율을 정확히 측정 할 수 있는 MR 기법을 개발하고자 하였다.

**대상 및 방법**: 쥐의 간세포를 분리하여 낸 후 NMR 측정을 시도하였다. 모든 실험은 0.02 MHz부터 60 MHz까지 양성자의 Larmor 주파수를 변화시킬 수 있는 IBM 형 field cycling relaxometer를 사용하여 시행하였으며 spin-echo 펄스열을 사용하여 T1 자기이완시간을 측정하였다. 저농도의 간특정 조영제인 Gd-EOB-DTPA를 함유하고 있는 간세포 샘플로부터 획득된 T1 데이터를 연속분포 분석법을 사용하여 분석하였으며 이때 이론적 모델로는 Two compartmental exchange 모델을 이용하였다.

**결 과**: 간세포내의 물분자의 평균 거주시간은 약 250 msec 이며 간세포막의 투과율에 대한 최저치는 $(1.3 \pm 0.1) \times 10^{-3}$cm / sec 이었다. 자기이완시간의 연속적인 분포도를 구할 수 있는 CONTIN 분석기법을 적용한 결과 확산적 물분자 교환이 일어남을 밝혔고 이러한 확산적 교환의 정도가 간세포의 경우 세포내 공간에서는 작지 않다는 사실을 규명 할 수 있었다.

**결 론**: 연속분포 분석기법을 적용하는 경우 Gd-EOB-DTPA는 간세포에서의 물분자의 교환정도 및 세포막의 물분자에 대한 투과율을 측정하는데 매우 유용한 방법임을 확인하였고 간세포에서의 물분자의 교환속도는 적혈구에서의 물분자 교환 속도에 비해 매우 느리다는 사실을 확인하였다. 따라서 조직 특정 조영제는 해당 조직 혹은 세포의 세포막 투과율과 같은 생리학적 정보를 알아낼수 있는 기능적 조영제로서의 유용성을 입증 할 수 있었다.

통신저자: 장용민 대구광역시 중구 삼덕동 50 경북대학교병원 진단방사선과
Tel. 82-053-420-5471 Fax. 82-53-422-2677